

## Effect of Chemical Composition and Isothermal Treatment Duration on Nano-bainite Steels

Jie DU<sup>1</sup>, Xiaobin ZHU<sup>1</sup>, Xingfu WANG<sup>2</sup>, Zhengcun ZHOU<sup>1\*</sup>

<sup>1</sup> School of Mechano-Electronic Engineering, Suzhou Vocational University, Suzhou, Jiangsu 215104, China

<sup>2</sup> Hefei Institute of Physical Science, Chinese Academy of Sciences, Hefei, Anhui 230032, China

<http://dx.doi.org/10.5755/j02.ms.38607>

Received 30 August 2024; accepted 13 February 2025

The effect of chemical composition and isothermal treatment duration on nano-bainite steels is investigated in this work. The steels that contain Co, V and Al elements with high C are designed and produced. The nano-bainite microstructures can be obtained by isothermal treatment in the Co and Al co-alloyed sample. Its mechanical properties and wear resistance performance are tested. Its microstructures were detected using a FESEM. After the steel is austenitized at 950 °C for 30 minutes and is subsequently isothermally treated at 260 °C for 2 hours, the nano-bainite structures can be obtained, whose microstructures also contain martensite and residual austenite in addition to nano-bainite. The isothermal time of 120 minutes is enough to obtain sufficient nano-bainite, which forms due to the addition of both Al and Co, which accelerate the austenite → bainite transformation, since Al and Co increase the free-energy difference between ferrite and austenite and the reaction rate for obtaining nano-bainites. The fracture toughness of the nano-bainite steel obtained by the isothermal transition is obviously better than the quenching + tempering steel for the Co and Al co-alloyed sample. The fracture morphology of the Charpy impact test shows that the fracture is ductile. Although nano-bainite steel has poor wear-resistance performance the initial stage compared to quenching + tempering steel, it shows more and more wear resistance performance with increasing wear time.

**Keywords:** nano-bainite steel, short isothermal transition time, wear-resistance performance.

### 1. INTRODUCTION

The ultra-fine bainitic steels with nano-bainite structures received much attention, since the ultra-fine bainitic structure was obtained in bainitic steels by Bhadeshia [1–6]. On the one hand, there are many factors that influence the bainitic transformation, which include chemical compositions [7–10], heat treatments [6, 11–13], deformation conditions [5, 14, 15], etc. On the other hand, there are complicated service conditions related to various microstructures of bainitic steels. Therefore, there is more controversy than any other transformation for the bainitic steels in physical metallurgy field due to its complexity [6, 16]. For example, the addition of niobium has been found to retard the bainitic transformation, while molybdenum addition effectively promoted the bainitic reaction in low-carbon bainite steels. A finer bainite microstructure was obtained in the austempered specimen below martensite start temperature ( $M_s$ ) compared to the specimen held above  $M_s$  [6].

It is known that low carbon bainitic steels possess ultrahigh strength [2, 4] and the bainitic steels with high C content have high hardness [7]. Generally, the former has lower hardness and bad wear-resistance and the latter has low toughness. Nano-bainitic steels possess high strength and hardness, good wear-resistance and good toughness. However, generally, nano-bainite can only be obtained by the isothermal transformation at lower martensite start temperature for a long time from days to months [7]. The long transformation time and expensive alloying elements

hinder the utilization of the ultra-fine bainitic steels in industry [1, 2, 7, 17]. Therefore, it is necessary to develop a nano-bainitic steel with high strength, good toughness and good wear-resistance by the isothermal transformation for short time and low alloying.

It is known that alloying elements have great effects on the bainitic transformation and silicon (Si) is a strongly promoter of graphitization and can effectively hinder the formation of cementite precipitation. Around 2 wt.% of silicon is added to inhibit cementite precipitation, which is a void nucleation phase that is detrimental to the impact properties of bainitic steels, producing carbide-free mixture microstructures of bainitic ferrite and carbon-riched retained austenite. The V element can control the primary austenite grains [4]. Elements such as Co and Al increase the stability of ferrite with respect to austenite, thus accelerating its formation, while Mn and C increase the stability of austenite [17]. The addition of Al and the reduction of Mn were used to accelerate the bainitic reaction [2]. Mn can also suppress the precipitation of both cementite and sulphide. Mo addition can improve hardenability and inhibit tempering brittleness. Cr is known as a ferrite stabilizer and it has a minimal effect on the free energy difference between austenite and ferrite and hence does not positively influence the bainitic transformation kinetics [2]. In this investigation, the chemical compositions of high C, high Si and medium Mn are selected with the additions of some Co and Al. On the one hand, the aim is to increase the free energy difference between ferrite and austenite and to accelerate the reaction rate and to reduce the bainitic transformation time. On the other hand, the nano-bainitic steels with high strength/high toughness and high hardness/good wear-resistance can be

\* Corresponding author: Z.C. Zhou  
E-mail: [zcc@jssvc.edu.cn](mailto:zcc@jssvc.edu.cn)

obtained. The general goals of the present research are to obtain a nanobainitic steel with high mechanical properties and wear resistance, as well as to reduce the isothermal transformation time by simultaneously alloying the steel with Co and Al.

## 2. EXPERIMENTAL PROCEDURES

Steel ingots with different chemical compositions (seen in Table 1) were prepared using a ZG-50 vacuum induction furnace under Ar-protection and the ingots are hot-forged at 1100 °C into a rectangle. The No.1 alloy compositions are designed according to Ref. 9 to compare with the No. 3 alloy and the former compositions are approximate to the compositions (0.98C-1.46Si-1.89Mn-0.26Mo-1.26Cr-0.09V wt.%, bal. Fe) in Ref. 9. These ingots are cut with a dimension of 100 × 40 × 40 mm. The rectangle samples are homogenized at 1200 °C for 12 hours, making the compositions of the samples uniform. All specimens are cut from the rectangle samples, having various sizes. Subsequently, the specimens are heated to 950 °C for 30 minutes, then cooled rapidly to 260 °C kept for 2 hours and 2.5 hours, respectively in nitrate-nitrite salt-bath furnace, at which the bainite transformation step is completed. In addition, the other specimens are quenched from 950 °C into water and then tempered at 260 °C for 2 hours, as shown in Fig. 1. All three specimens are heat treated by the same method.

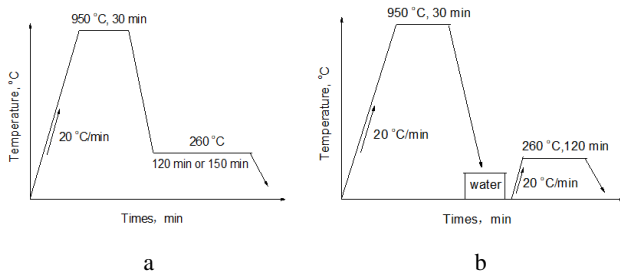


**Fig. 1.** Schematic diagram of the heat treatment process: a – isothermal transformation; b – quenching+tempering

The mechanical properties ( $\sigma_b$ ,  $\sigma_{0.2}$ ,  $\delta$ ,  $\Psi$ , where  $\sigma_b$  is tensile strength and  $\sigma_{0.2}$  is conditional yield strength,  $\delta$  is the elongation and  $\Psi$  is the reduction of the cross-section area) of flat tensile test are measured with gauge lengths of 25 mm according to the ASTM E8-09 standard method which were cut in the forging direction. The specimen size of the tensile test is  $\varnothing 5 \times 25$  mm. The Charpy impact test specimens are prepared with a U-notch shape with a dimension of 10 × 10 × 55 mm in which notches are perpendicular to the forging direction. The impact tests are implemented at room temperature and -50 °C according to

**Table 2.** The mechanical properties of three specimens with different heat treatments

| Heat treatment procedure          | Specimen No. | $\sigma_b$ , MPa | $\sigma_{0.2}$ , MPa | $\delta$ , % | $\Psi$ , % | Impact energy KU2, J |          | HV2    |
|-----------------------------------|--------------|------------------|----------------------|--------------|------------|----------------------|----------|--------|
|                                   |              |                  |                      |              |            | 20 °C                | -50 °C   |        |
| Isothermal transformation 2 hours | 1            | 1128±50          | 1073±50              | 16±2         | 66±4       | 67.7±10              |          | 553±20 |
|                                   | 2            | 1118±50          | 1062±50              | 14±2         | 64±4       | 66.6±10              |          | 549±20 |
|                                   | 3            | 1132±50          | 1079±50              | 16±2         | 64±4       | 147.1±10             | 102.7±10 | 560±20 |
| Quenching + tempering             | 1            | 1411±50          | 1335±50              | 11.5±2       | 55±4       | 49.7±10              |          | 545±20 |
|                                   | 2            | 1434±50          | 1327±50              | 10±2         | 53±4       | 53.5±10              |          | 537±20 |
|                                   | 3            | 1438±50          | 1354±50              | 13±2         | 56±4       | 107±10               | 69±10    | 559±20 |

the ASTM E23-07 standard. Three tests are performed for each specimen, and the average value is taken at the end. The wear test is finished on dynamic load grinding material wear testing machine MLD-10 tester (Xuanke Testing Machine Manufacturing Company in China) and the specimen sizes are 10 × 10 × 40 mm, polished by 1200 grit silicon carbide sandpaper. The impact absorption energy of the hammer is 4 J, and the impact frequency is set to 100 times/min, the abrasive size is quartz with a particle size less than 0.4 mm, with a corresponding flow rate of 6 g/s. The duration of a single test is 50 minutes. All mechanical experiments are repeated five times for the identical specimen. The wear experiments of the No. 3 specimen with different isothermal transforming time are carried out. The presented values in Table 2 were the average values, obtained after 3 tests. In addition, the wear tests are also completed. In addition, the wear mass of the No. 3 specimens with different isothermal transformation time (5, 30, 90, 120, 180, 360 minutes) are also tested.

The specimens for microscopic examination and hardness measurements have a dimension of 10 × 10 × 5 mm are polished and etched using 4 % nitrate alcohol solution. The FESEM (Field Emission Scanning Electron Microscopy) is used to observe the microstructures of the No. 3 specimens with different IT time. The hardness values of the specimens with a size of 10 × 5 × 5 mm are measured using a Japan FTFM-700 hardness tester. The load is 2 kg (1.96 N) and the hold time is 60 s. Each specimen is tested 3 times, and the average value is taken at the end.

**Table 1.** The tested steel with three chemical compositions, wt.%

| Alloy | C    | Si   | Mn   | Mo   | Cr   | V    | Co   | Al   | Fe   |
|-------|------|------|------|------|------|------|------|------|------|
| 1     | 0.95 | 1.46 | 1.92 | 0.23 | 1.05 | 0.10 |      |      | Bal. |
| 2     | 0.85 | 1.49 | 1.90 | 0.26 | 0.98 |      | 1.56 |      | Bal. |
| 3     | 0.78 | 1.45 | 1.88 | 0.22 | 1.03 |      | 1.62 | 0.97 | Bal. |

In addition, the bainitic ferrite volume of the three IT specimens with different isothermal transformation time at 200 °C, 250 °C, 300 °C is investigated and estimated by observation of FESEM, respectively.

## 3. RESULTS AND DISCUSSION

The chemical compositions of the tested steels are detected using a chemical analysis method as shown in Table 1. The mechanical properties of three specimens with different heat treatments are listed. In Table 2,  $\sigma_b$  is the tensile strength and  $\sigma_{0.2}$  is the conditional yield strength;  $\delta$  is the elongation and  $\Psi$  is the reduction of area. KU2 is impact energy and HV is Vickers hardness.

From Table 2, it can be seen that the No. 3 specimens have the best mechanical properties under both of IT and QT states among the three steels, indicating that a single Co element has no effect on the improvement of the mechanical properties for both isothermal transformation (abbreviated as IT, as the same below) and quenching + tempering (abbreviated as QT, as the same below) treatments. Also, it can be noticed that both yield strength and tensile strength of the IT specimens are smaller than those of the QT specimens with the same compositions and both elongation and reduction rates are exactly opposite. Nevertheless, the former of the product of strength and plasticity is larger than the latter, indicating that the toughness of the former is better than the latter. In particular, the low-temperature impact toughness value of the No. 3 IT specimen is obviously larger than those of the No. 3 QT specimen. The IT specimens have a higher hardness than the QT specimens with the compositions.

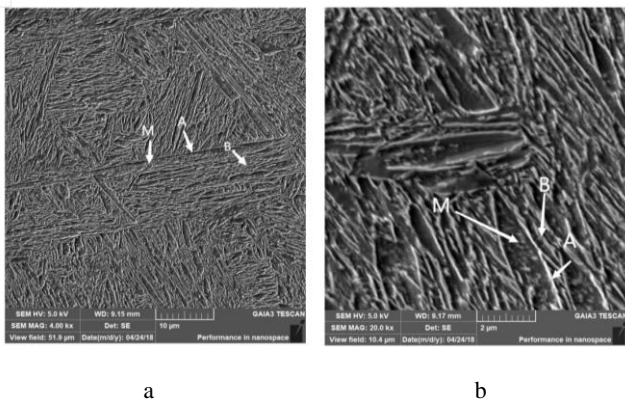


**Fig. 2.** The SEM images of the No. 3 IT specimen for isothermal transformation 120 minutes with different magnification: a –  $4 \times 10^3$  times; b –  $20 \times 10^3$  times

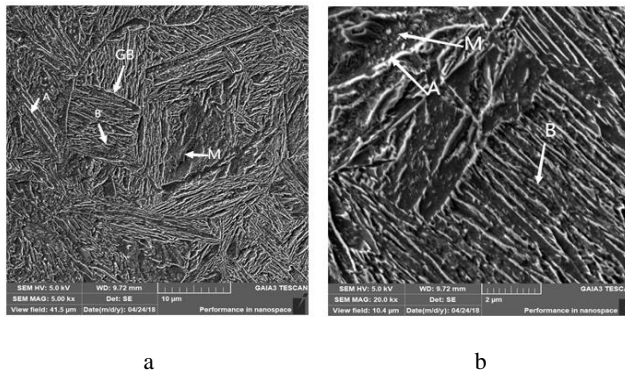


**Fig. 3.** The SEM images of the No. 3 IT specimen for isothermal transformation 150 minutes at 260 °C with different magnification: a –  $5 \times 10^3$  times; b –  $20 \times 10^3$  times

Fig. 2 shows the FESEM images of the IT specimen No. 3. Its microstructures consist of nano-bainite and a few residual austenite grains and a little martensite. Fig. 3 the SEM images of the No. 3 IT specimen for isothermal transformation 150 minutes at 260 °C. There are no obvious differences in their structures and volume of nano-bainite with a size of about 200–300 nm and residual austenite for the two specimens. The IT time is drastically reduced compared to the alloy in Ref. 7 and Ref. 9, whose IT time is several days, indicating that the additions of Al

and Co elements accelerate evidently the austenite → bainite transformation. From Fig. 2 a and Fig. 3 a, it can be noticed that the microstructure of the isothermally treated No. 3 specimen for 2.5 hours is coarser than the one for 2 hours, possibly resulted from longer transforming time or inhomogeneous distribution in microstructures of bainite, austenite and martensite. Obviously, the thin bainitic plates were separated with austenite microblocks and each sheaf consisted of parallel layers of bainitic ferrites and austenite films. Carbon rejects from bainitic ferrite to surrounding austenite during the bainite transformation and bainite formation stops when the austenite carbon content reaches that predicted by the T<sub>0</sub> diagram [9], whose results are like the reports in Ref. 4. The center region of the latter is especially poor in carbon content, which would lead to higher thermal and mechanical stability of filmy morphology compared to that of blocky austenites according to Ref. 4 and Ref. 18 and therefore the center regions of the austenite blocks tend to transform to martensite during cooling to room temperature at the end of the bainite transformation.

The SEM image of fracture surface of the Charpy impact test is shown in Fig. 4. The type of fracture is ductile fracture. From Table 2, it can be seen that the absorbed impact energy of the No. 3 QT/IT specimens is about two times that of the No. 1 and No. 2 QT/IT specimens, respectively. The detailed mechanisms have not been cleared.

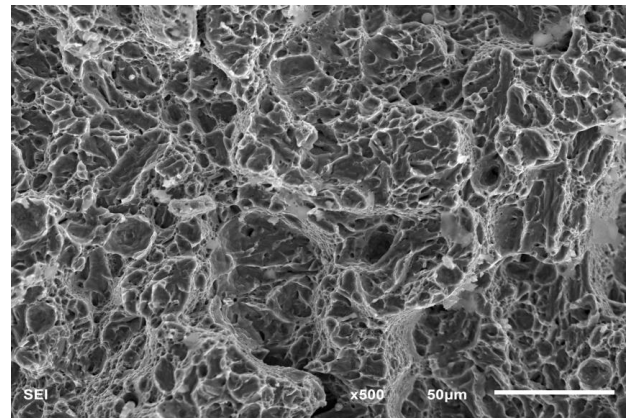


**Fig. 4.** The SEM image of the fracture surface of the Charpy impact test for No. 3 IT specimen

The nano-bainite can be obtained using a short isothermal transformation time which originates from the effect of Al and Co. Al enhances the kinetics of the bainite transition. For high carbon bainitic steel, aluminum can sharply accelerate isothermal bainitization under low temperature conditions, which is confirmed by the results in Fig. 5. The addition of Al and Co elements decrease the transformation time of austenite → bainite for No. 3 alloy, as shown in Fig. 5.

From Fig. 5, it can be seen that the present bainitic ferrite fraction is about 70 % for the No. 3 IT specimen at 250 °C. According to the T<sub>0</sub> diagram in Ref. 9 and Ref. 19, carbon content is estimated to be about 1.04 % for the residual austenite.

Fig. 6 shows the variation of wear mass at different isothermal transformation time for No. 3 alloy with wear time.

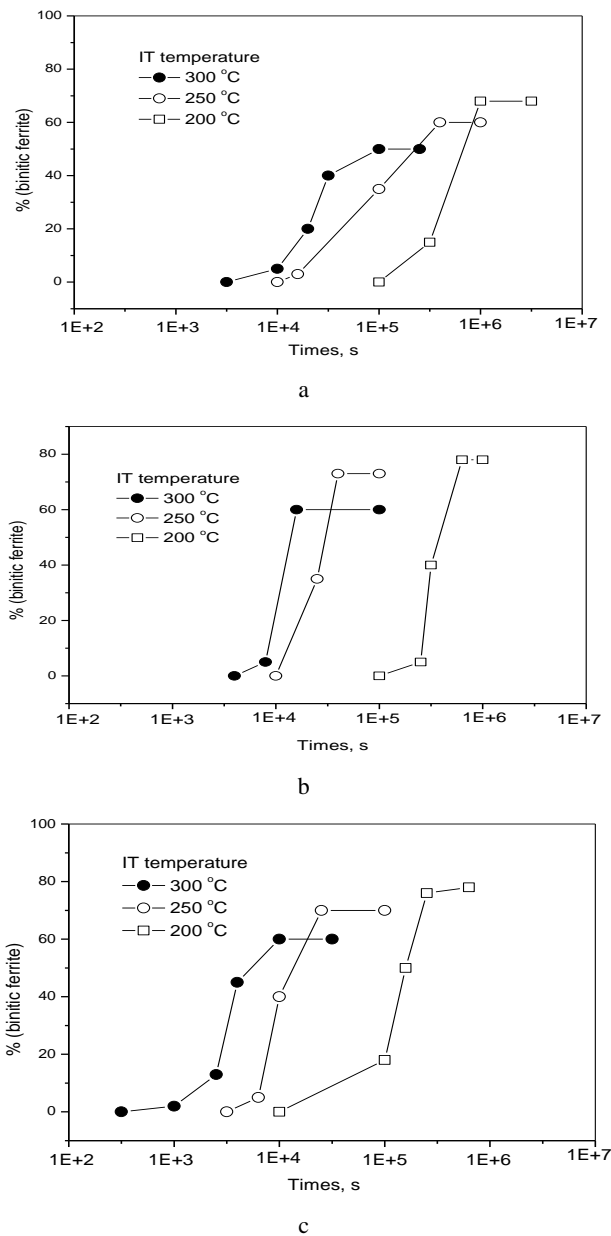


**Fig. 5.** The relationship between the bainitic ferrite fraction of the bainite isothermal transformation (IT) time and temperature of the three steels for IT specimens: a - alloy 1; b - alloy 2; c - alloy 3

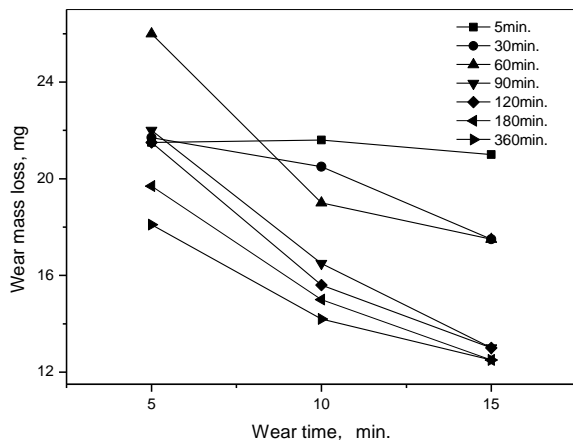


**Fig. 6.** The variation of wear mass at different isothermal transformation time for No. 3 specimen with wear time

From Fig. 6, it can be seen that the wear mass of the specimens with the shorter isothermal transformation time has higher values than that of the specimens with the longer isothermal transformation time. Nevertheless, too long isothermal transformation time has no great effect on decreasing wear mass. Therefore, the isothermal transformation time of 120 minutes is enough to obtain the nano-bainites and decrease the wear mass. There is little difference in wear performance and microscopic distinction for two IT times of 120 minutes and 150 minutes from Fig. 2, Fig. 3, and Fig. 5.

Fig. 7 shows the variation of the wear mass of the IT specimens with different compositions with the wear time. From Fig. 7, it can be seen that the wear mass of No. 1 IT specimen initially is lowest and that of the No. 3 IT specimen is highest among three alloys. Nevertheless, the wear mass of the No. 3 IT specimen is reduced with increasing the wear time, indicating that the wear resistance of the No. 3 IT specimen increases compared to the other two alloys.

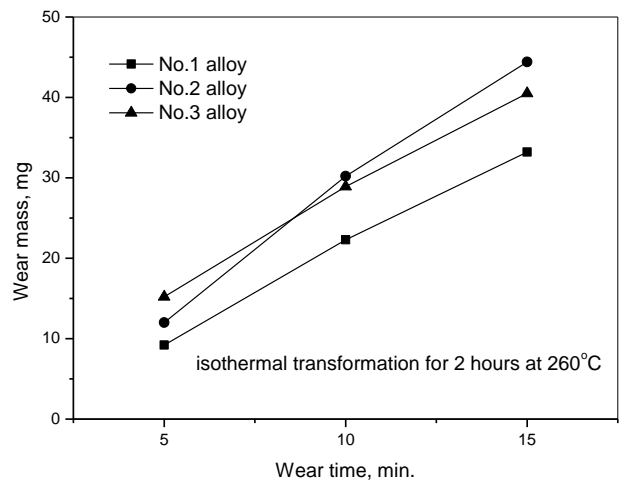


**Fig. 7.** The variation of wear mass of the IT specimens with different compositions with the wear time

The main focus is on studying the trend of wear of different samples over time in Fig. 6 and therefore the standard deviation and the confidence intervals are not given, which do not influence the discussion of relevant results. This is also true in other parts of the present investigation.

From Fig. 8, it can be seen that the wear mass of the QT No. 3 specimen with martensite is initially smaller than that of the No. 3 IT specimen with nano-bainite.

Nevertheless, the wear rate of the former increases and that of the latter decreases after 250 minutes wear test, which is attributed to the martensitic structure in the No. 3 QT specimen. The wear rate decrease of the latter at later stage is attributed to the refined nano-microstructure and the austenite  $\rightarrow$  martensite transformation induced plasticity (TRIP) effect during the wear process in nano-bainitic steel [1]. The retained austenite in the IT specimen will transform into martensite, which increases wear resistance.

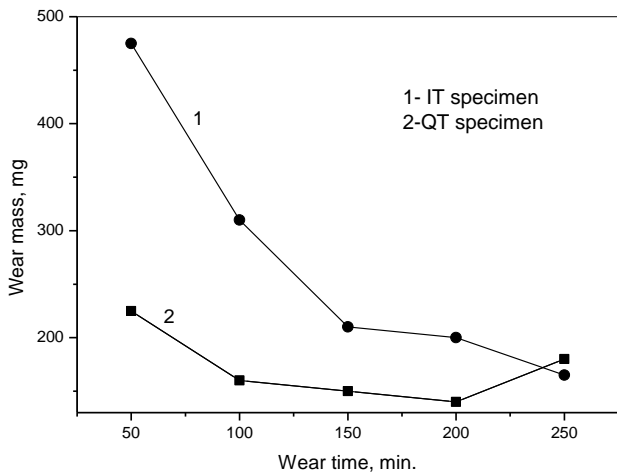


**Fig. 8.** The wear rate variation of the No.3 specimens with different heat treatments with wear time

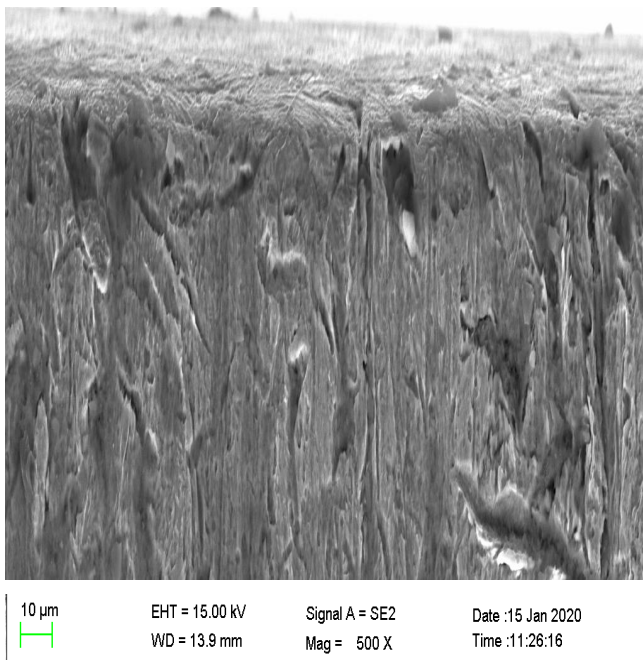


**Fig. 9.** The SEM image of surface morphology of the worn surface of nano-bainitic steel for No. 3 IT specimen

#### 4. CONCLUSIONS

The nano-bainite steel can be obtained by the isothermal transformation and the isothermal transformation time is decreased by the addition of Al and Co. The nano-bainite steel contains martensite and residual austenite in addition to nano-bainite. The impact energy of the nano-bainite steel obtained by the isothermal transition is obviously better than the quenching + tempering steel at low temperature for the Co and Al co-alloyed specimen. The fracture morphology of Sharp impact test shows the fracture is ductile. Additionally, the Co and Al co-alloyed IT specimen possesses the best tensile strength among all specimens and its plasticity is a little worse than the Co and Al co-alloyed QT specimen.

At the initial wear stage, the wear mass of the Co and Al co-alloyed IT specimen is about 2.1 times of the Co and Al co-alloyed QT specimen for 50 minter-wear-test and

while the wear mass of the Co and Al co-alloyed IT specimen is about 0.91 times of the Co and Al co-alloyed QT specimen for 250 minute-wear-test.

#### Acknowledgments

This work was supported by Natural Science Foundation of the Jiangsu Higher Education Institutions of China (22KJB150038, 23KJB430034) and Qinglan Project of Jiangsu Province of China (202305000008) and Guangdong University of Science and Technology Research Ability Enhancement Project (GKY-2022ZDXKTS-4).

#### REFERENCES

- Ríos-Diez, O., Aristizábal-Sierra, R., Serna-Giraldo, C., Jimenez, J.A.** Development of Nanobainitic Microstructures in Carbo-austempered Cast Steels: Heat Treatment, Microstructure and Properties *Metals* 10 (5) 2020: pp. 635. <https://doi.org/10.3390/met10050635>
- Mohamad, A., Heinz, P., Mohamed, S.** High-Strength Low-Cost Nano-Bainitic Steel *Journal of Material Engineering and Performance* 29 (4) 2020: pp. 2418–2427. <https://doi.org/10.1007/s11665-020-04771-4>
- Baradari, S., Boutorabi, S.M.A.** Microstructural Assessment of Nanobainite formed in a Chemically Heterogeneous High-Carbon Al-Si Alloyed Steel *Journal of Metastable and Nanocrystalline Materials* 34 2022: pp. 1–18. <https://doi.org/10.4028/p-C6mbeN>
- Mousalou, H., Yazdani, S., Ahmadi, N.P., Avishan, B.** Nanostructured Carbide-Free Bainite Formation in Low Carbon Steel *Acta Metallurgica Sinica* 33 (12) 2020: pp. 1635–1644. <https://doi.org/10.1007/s40195-020-01091-3>
- Wang, Y.H., Sun, H.Q., Feng, W.J., Zhao, L.J., Chen, X., Chen, Q.A., Sun, H.T., Wang, J.J., Yang, Z.N.** Notably Accelerated Nano-Bainite Transformation via Increasing Undissolved Carbides Content on GCr15Si1Mo Bearing Steel *Acta Metallurgica Sinica* 37 2024: pp. 703–712. <https://doi.org/10.1007/s40195-023-01652-2>
- Liu, M., Xu, G., Tian, J., Yuan, Q., Chen, X.** Effect of Austempering Time on Microstructure and Properties of a Low-carbon Bainite Steel *International Journal of Minerals, Metallurgy and Materials* 27 (3) 2020: pp. 340–346. <https://doi.org/10.1007/s12613-019-1881-y>
- Garcia-Mateo, C., Caballero, F.G., Bhadeshia, H.K.D.H.** Development of Hard Bainite *ISIJ International* 43 (8) 2003: pp. 1238–1243. <https://doi.org/10.2355/isijinternational.43.1238>
- Caballero, F.G., Bhadeshia, H.K.D.H.** Design of Novel High-strength Bainitic Steels *Materials Science Forum* 426 (4) 2003: pp. 1337–1342. <https://doi.org/10.4028/www.scientific.net/MSF.426-432.1337>
- Bhadeshia, H.K.D.H.** High Performance Bainitic Steels *Science Forum* 500–501 2005: pp. 63–74. <https://doi.org/10.4028/www.scientific.net/MSF.500-501.63>
- Kirbiš, P., Anžel, I., Rudolf, R., Brunčko, M.** Novel Approach of Nanostructured Bainitic Steels Production with

- Improved Toughness and Strength *Materials* 13 (5) 2020: pp. 1220.  
<https://doi.org/10.3390/ma13051220>
11. **Han, B., Chen, L., Wu, S.J.** Effect of Austempering-Partitioning on the Bainitic Transformation and Mechanical Properties of a High-Carbon Steel *Acta Metallurgica Sinica (English Letter)* 28 (5) 2015: pp. 614–618.  
<https://doi.org/10.1007/s40195-015-0239-3>
  12. **Zhou, Z.C., Wang, S.Z., Li, J.S., Li, Y.S., Wu, X.L.** Hardening after Annealing in Nanostructured 316L Stainless Steel *Nano Materials Science* 2 2020: pp. 80–82.  
<https://doi.org/10.1016/j.nanoms.2019.12.003>
  13. **Yang, Z.N., Chu, C.H., Jiang, F., Qin, Y.M., Long, X.Y., Wang, S.L., Chen, D., Zhang, F.C.** Accelerating Nano-Bainite Transformation Based on a New Constructed Microstructural Predicting Model *Materials Science Engineering A* 748 2019: pp. 16–20.  
<https://doi.org/10.1016/j.msea.2019.01.061>
  14. **Gong, W., Tomota, Y., Adachi, Y., Paradowska, A.M., Kelleher, J.F., Zhang, S.Y.** Effects of Ausforming Temperature on Bainite Transformation, Microstructure and Variant Selection in Nanobainite Steel *Acta Materialia* 61 (11) 2013: pp. 4142–4154.  
<https://doi.org/10.1016/j.actamat.2013.03.041>
  15. **He, J.G., Zhao, A.M., Zhi, C., Fan, H.L.** Acceleration of Nanobainite Transformation by Multi-step Ausforming Process *Scripta Materialia* 107 2015: pp. 71–74.  
<https://doi.org/10.1016/j.scriptamat.2015.05.023>
  16. **Borgenstam, A., Hillert, M., Ågren, J.** Metallographic Evidence of Carbon Diffusion in the Growth of Bainite *Acta Materialia* 57 (11) 2009: pp. 3242–3252.  
<https://doi.org/10.1016/j.actamat.2009.03.026>
  17. **Caballero, F.G., Bhadeshia, H.K.D.H.** Very Strong Bainite *Current Opinion in Solid State and Materials Science* 8 (3–4) 2004: pp. 251–257.  
<https://doi.org/10.1016/j.cossms.2004.09.005>
  18. **Van Dijk, N., Butt, A., Zhao, L., Sietsma, J., Offerman, S., Wright, J., Van der Zwaag, S.** Thermal Stability of Retained Austenite in TRIP Steels Studied by Synchrotron X-ray Diffraction during Cooling *Acta Materialia* 53 (20) 2005: pp. 5439–5447.  
<https://doi.org/10.1016/j.actamat.2005.08.01>
  19. **Babu, S.S., Specht, E.D., David, S.A., Karapetrova, E., Zschack, P., Peet, M., Bhadeshia, H.K.D.H.** In-Situ Observations of Lattice Parameter Fluctuations in Austenite and Transformation to Bainite *Metallurgical and Materials Transactions A* 36A (12) 2005: pp. 3281–3289.  
<https://doi.org/10.1007/s11661-005-0002-x>



© Du et al. 2025 Open Access This article is distributed under the terms of the Creative Commons Attribution 4.0 International License (<http://creativecommons.org/licenses/by/4.0/>), which permits unrestricted use, distribution, and reproduction in any medium, provided you give appropriate credit to the original author(s) and the source, provide a link to the Creative Commons license, and indicate if changes were made.